Adsorption of Di- and Tripeptides on Au(110) under Ultrahigh Vacuum Conditions. 1. Polarization Modulation Reflection Absorption Infrared Spectroscopy and X-ray Photoelectron Spect...

ARTICLE *in* THE JOURNAL OF PHYSICAL CHEMISTRY C · MAY 2009

Impact Factor: 4.77 · DOI: 10.1021/jp9003888

4 AUTHORS, INCLUDING:

Anne Vallée
Université de Versailles Saint-Quentin
15 PUBLICATIONS **285** CITATIONS
SEE PROFILE

Vincent Humblot
Pierre and Marie Curie University - Paris 6
57 PUBLICATIONS **1,327** CITATIONS
SEE PROFILE

Claire-Marie Pradier
Pierre and Marie Curie University - Paris 6
170 PUBLICATIONS **2,816** CITATIONS
SEE PROFILE

Adsorption of Di- and Tripeptides on Au(110) under Ultrahigh Vacuum Conditions. 1. Polarization Modulation Reflection Absorption Infrared Spectroscopy and X-ray Photoelectron Spectroscopy Characterization

Anne Vallée, Vincent Humblot, Christophe Méthivier, and Claire-Marie Pradier*

Laboratoire de Réactivité de Surface, UMR CNRS 7609, Université Pierre et Marie Curie, 4 place Jussieu, Case 178, 75252 Paris Cedex 05, France

Received: January 14, 2009; Revised Manuscript Received: February 24, 2009

Two tripeptides, insulin-like growth factor I (IGF) (1−3) and gluthation (GSH), only differing by their central fragment, and one IGF-related dipeptide, Gly-Pro, were adsorbed on a Au(110) surface under UHV conditions. Studies of the kinetics of adsorption, as well as the chemical and structural characterization of the adlayers, were achieved by combining polarization modulation reflection absorption infrared spectroscopy and X-ray photoelectron spectroscopy techniques. Low-energy electron diffraction observations are also reported. The adsorption behavior varies drastically with the size and chemical composition of these three molecules. Gly-Pro, constituted of two of the three amino acids of IGF, adsorbs on the Au(110) surface, giving rise to a 2D organization and rapidly forming a full monolayer. The two tripeptides only differ by their central fragment and this modifies their growth mode drastically: IGF tends to form homogeneous, likely continuous, layers, while GSH adsorption results in heterogeneous layers with dimers or patches of molecules, leaving fractions of the gold surface bare or covered with a very thin layer of organics. Moreover, the average thickness of the IGF layer of on Au (110) increases faster than that of GSH with exposure time. The adsorption kinetics is faster for IGF than for GSH.

Introduction

The adsorption of biomolecules or biorelated molecules on metal surfaces, analyzed by advanced surface science techniques, is a relevant topic nowadays, leading to the understanding of the interface phenomenon in biomaterials, biochemistry, or pharmacology industries.[1] In the last 10 years, adsorptions of amino acids on metal surfaces have been much studied to understand the various modes of adsorption, the 2D surface organization, and the fundamental aspect of the interactions between a surface and a biomolecule.[2–7] These studies are the precursor to understanding how peptides interact with the surfaces.

More recently, adsorption of more complex biomolecules, such as peptides, has been studied on metal surfaces most of the time from the liquid phase.[8–12] Studies of peptides are a step closer toward "real biology".

Adsorption of polypeptides under controlled ultrahigh vacuum (UHV) conditions is another challenge. Up to date, to our knowledge, only two studies have been done under UHV conditions. In the first one, two homo tripeptides, tri-L-alanine and the tri-L-leucine, had been adsorbed onto Cu(110) and studied using reflection−absorption infrared spectroscopy (RAIRS) and low-energy electron diffraction (LEED).[13] The second one was a scanning tunnelling microscopy (STM) study of the di-L-phenylalanine adsorption on Cu(110) and Cu(100).[14] These molecules are of ca. 200−300 amu and are constituted of several amino acids fragments that can interact with the surface. The questions are, once they are sublimated in the vacuum chamber (10^{-10}Torr), (i) do they adsorb as intact molecules, (ii) which is (are) the group(s) that interact with the surface, and (iii) what is the adlayer structure? We have recently characterized the adsorption of gluthation (GSH) on Au(111) under UHV conditions[15,16] and showed that the adsorption occurs mostly via the sulfur atoms and that the growth occurs via the creation of dimers or small aggregates rather than as a uniform layers. The presence of sulfur on the cysteine fragment appears to be determining.

In the present work, we report the adsorption, on a rather open surface, Au(110), of two quite similar tripeptides, GSH (γ-Glu-Cys-Gly) and insulin-like growth factor I (IGF, Gly-Pro-Glu), presented in Figure 1a,b, and of a dipeptide, the Gly-Pro (see Figure 1c), chosen to help illuminate IGF adsorption. The two tripeptides mainly differ by the central amino acid, cysteine in the case of GSH and proline in the case of IGF.

The experiments were carried out under UHV conditions at room temperature and characterized by means of three surface science techniques: polarization modulation reflection absorption infrared spectroscopy (PM-RAIRS), X-ray photoelectron spectroscopy (XPS), and LEED.

Experimental Section

Materials. L-Glutathione (≥98%), from Sigma-Aldrich Inc., and IGF-I (1−3) and Gly-Pro, from Bachem, were used as received; the peptide was deposited in a small glass tube and heated by a system of electrodes which is inserted and can be placed in the UHV chamber very close to the surface. The evaporator was initially separated from the main chamber by a gate valve and differentially pumped by a turbomolecular pump. Before sublimation, the GSH, IGF, or Gly-Pro powder was outgassed at 370 K. It was then heated to 400 K and introduced in the chamber, where the glass tube was placed in front of the gold crystal.

* To whom correspondence should be addressed. E-mail: claire-marie.pradier@upmc.fr.

10.1021/jp9003888 CCC: $40.75
Published on Web 05/01/2009

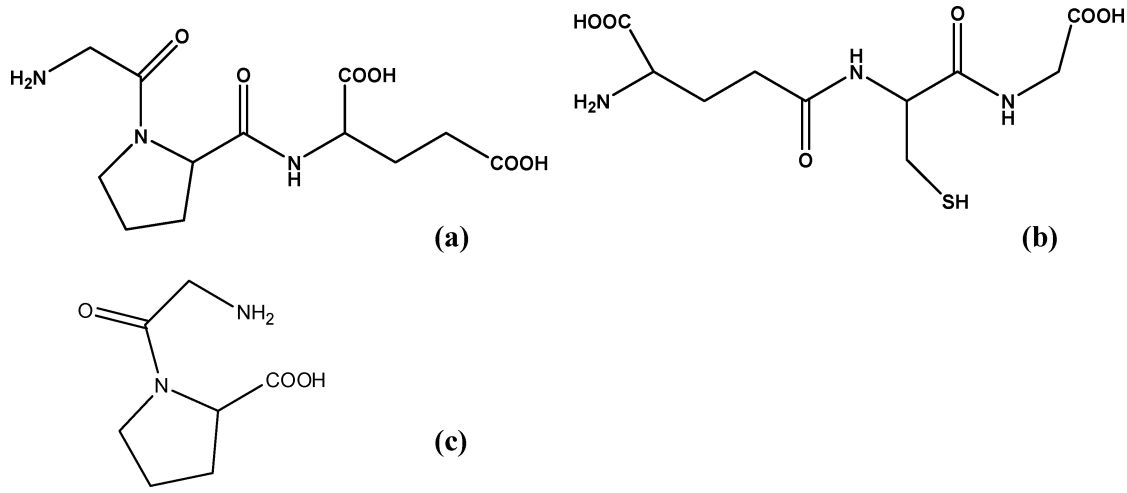

Figure 1. The three peptides molecules: (a) IGF (Gly-Pro-Glu), (b) GSH (γ-Glu-Cys-Gly), and (c) Gly-Pro.

In Situ PM-RAIRS Characterizations. PM-RAIR spectra were recorded using a Nicolet 5700 spectrometer equipped with a nitrogen-cooled MCT wide-band detector. A ZnSe grid polarizer and a ZnSe photoelastic modulator to modulate the incident beam between p and s polarization (HINDS Instruments, PEM 90, modulation frequency = 50 kHz) are placed prior to the sample. The spectrometer was interfaced to an UHV chamber with ZnSe windows. The reflected light is focused onto the detector at an optimal incident angle of 85°. The Au(110) single crystal was mounted in a multitechnique UHV chamber, with a base pressure of 1×10^{-10} Torr, with PM-RAIRS, LEED, Auger electron spectroscopy (AES), and XPS facilities. The gold crystal was cleaned by cycles of Ar^+ ion sputtering ($P_{Ar} = 2 \times 10^{-5}$ Torr, 250 V), flashing, and annealing to 850 K. The surface structure and cleanliness were monitored by LEED and AES before and after adsorption experiments.

XPS Analyses. For XPS analyses, once the GSH, IGF, or Gly-Pro vapor was evacuated down to a base pressure of 1×10^{-10} Torr, the sample was transferred to the adjacent UHV XPS chamber and cooled to 100 K before analysis. XPS spectra were collected on a SPECS (Phoibos MCD 150) X-ray photoelectron spectrometer, using a Mg Kα ($h\nu = 1253.6$ eV) X-ray source having a 150 W (12 mA, 12.5 kV) electron beam power. The emissions of photoelectrons from the sample were analyzed at a take-off angle of 90° under UHV conditions. High-resolution spectra were collected at a pass energy of 10 eV for C1s, O1s, N1s, Au4f, and S2p core XPS levels. No charge compensation was applied during acquisition.

After collection, the binding energies were calibrated against either the Au4f peak at a binding energy of 84.0 eV, when there was obviously no charging effect; another way of calibrating the binding energies was used in some cases, using the O1s peak; this will be described later in the Results. The XPS peak areas were determined after subtraction of a background. The atomic ratio calculations were performed after normalization using Scofield factors.[17]

For the analysis of XPS data, a model with a homogeneous layer of polypeptide was assumed to calculate the polypeptide thickness

$$\frac{I_C}{I_{Au}} = \frac{\sigma_C N_C \lambda_C \left(1 - \exp\left(-\frac{d}{\lambda_C}\right)\right)}{\sigma_{Au} N_{Au} \lambda_{Au} \exp\left(-\frac{d}{\lambda_{Au}}\right)}$$

where θ is the take-off angle of the photoelectrons with respect to the sample surface, σ_X is the photoionization cross section of element X, λ_X is the inelastic mean free path of the photoelectrons emitted by the X core level, d is the peptide thickness layer, and N is proportional to the density of the powder.

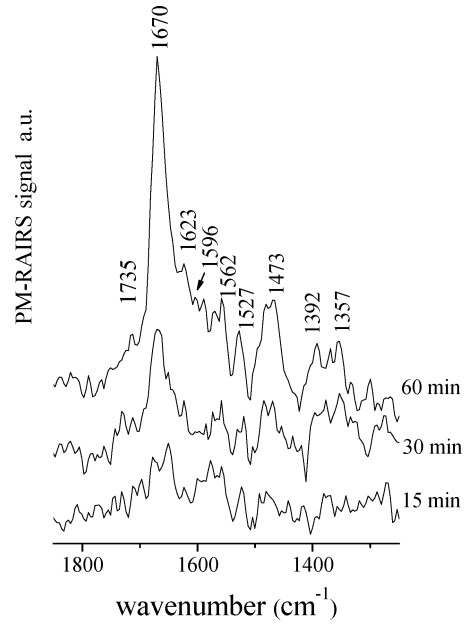

Figure 2. PM-RAIR spectra recorded upon increasing exposure of Gly-Pro at 300 K on Au(110).

All spectrum processing was carried out using the Casa XPS v2.3.13 software (Casa Software Ltd.) package and Origin 7.1 (Origin Laboratory Corp.). The spectral decomposition was performed by using Gaussian−Lorentzian (70%/30%) functions, and the fwhm is fixed for each given peak.

Results

Gly-Pro on Au(110). First, molecular Gly-Pro, a fragment of the IGF molecule, was adsorbed on Au(110). The PM-RAIR spectra of the Au(110) surface, recorded during Gly-Pro exposure ($P_{Dose} = 1 \times 10^{-8}$ Torr) are shown in Figure 2. After 15 min of exposure (lower spectrum), the peaks are not very intense but are well-defined. All bands increase with exposure, leading to the main following features: the most intense Gly-Pro-related bands, observed at 1670 cm^{-1}, are attributed to C═O amide I; bands at 1735 and 1357 cm^{-1} are assigned respectively to $\nu_{C=O}$ and ν_{C-O} of the carboxylic acid group;[18] and the bands

TABLE 1: Infrared Frequencies and Vibrational Assignments from the Spectra of Gly-Pro, IGF, and GSH Adsorbed on Au(110)

assignment	Gly-Pro	IGF	GSH
$\nu_{C=O}$	1735	1743	1731
$\nu_{C=O}$ H-bonded or amide I			1697
amide I	1670	1666	1650
$\delta_{as}^{NH_3^+}$	1623	1631	1631
$\nu_{as}^{COO^-}$	1596	1590	1581
amide II and/or δ^{NH_2}	1562	1554	1531
$\delta_{s}^{NH_3^+}$	1527	1527	
sciss CH_2 ring	1473	1488	
δ_{CH_2}		1442	1460
$\nu_{s}^{COO^-}$		1415	1415
ν_{C-O}	1392		1384
ν_{C-O}	1357	1353	1330

at 1596 and 1415 cm^{-1} are attributed respectively to the asymmetric and symmetric stretching of carboxylate groups.[19] This highlights that carboxylic acid and carboxylate groups are simultaneously present in the layer. In addition, the presence of weak absorption bands at 1623 and 1519 cm^{-1} may be ascribed to the asymmetric and symmetric deformations of NH_3^+ of some protonated amine groups,[20] and the band at 1562 cm^{-1} is assigned to the NH_2 deformation.[21] Eventually, the band at 1477 cm^{-1} is attributed to the CH_2 scissor of the aliphatic ring of proline.[19] All expected vibrations of the functionalities and the amide band of Gly-Pro are identified on the spectra, suggesting that Gly-Pro is adsorbed intact on the Au(110) surface.

When the coverage increases, after 60 min of exposure, the band at 1670 cm^{-1} becomes predominant; it mainly originates from the amide I vibrations. This band presents two shoulders at 1623 and 1596 cm^{-1}, attributed respectively to the asymmetric deformation of NH_3^+ and the asymmetric stretching of COO^-. Other peaks are identified, at 1527 and 1562 cm^{-1}, which may be assigned to the symmetric deformation of NH_3^+ and to the NH_2 deformation, respectively.[22] Moreover, the stretching mode of C═O of the carboxylic acid group at 1735 cm^{-1} has a very low intensity, suggesting that the majority of carboxylic acid groups are now deprotoned. A summary of the frequency assignments is given in Table 1.

A series of XPS spectra was recorded at ambient temperature for different exposure times of 3, 30, and 60 min. Figure 3 shows the C1s, O1s, and N1s region recorded after increasing exposure times, and Table 2 summarizes the main XPS data. Note first that when the coverage increases, all spectra are shifted due to a charge effect;[23] only the Au4f peak remains at the expected position of 84.0 eV; thus, the O1s contribution at low binding energy (531.7 eV), considered as well-representing the oxygen in COO^-, N−C═O groups of all molecules, was taken to recalibrate the C1s, N1s, and, of course, O1s peaks; with such a calibration, these peaks were shifted by 0.2 and 0.9 eV after 30 and 60 min of exposure, respectively. All values given in Table 2 have been corrected.

After 3 or 30 min of exposure, the C1s peak of Gly-Pro could be decomposed into four contributions at 285.0 ± 0.1, 286.0 ± 0.1, 287.9 ± 0.1, and 288.9 ± 0.1 eV, respectively assigned to the carbons in C−C or C−H bonds, C−N, N−C═O or COO^-, and COOH groups.[24] When the coverage is increased up to 60 min, the contribution of the COOH groups disappears, in agreement with the PM-RAIRS data, suggesting an almost complete deprotonation of the carboxyl groups at that coverage. Note that the relative amount of the C−C/C−H contribution decreases when increasing the exposure, and this has been observed for the three adsorbed molecules; this is probably due to the presence of carbonaceous contamination at low coverage; after 60 min, the C−C, C−H/C−N/C═O, COOH ratios are in agreement with the Gly-Pro molecule formula (2/3/2).

Two contributions are identified in the N1s peak of Gly-Pro, at 399.9 ± 0.1 and 401.3 ± 0.1 eV, corresponding, respectively, to the ternary N or N−H or NH_2 groups and to NH_3^+ groups.[25] Note that the NH_3^+ fraction increases with exposure time, as expected from the just mentioned simultaneous evolution of the C1s peak. The O1s peak shows two contributions at 531.4 ± 0.1 and 533.0 ± 0.1 eV, attributed respectively to the double-bonded oxygen of acidic and amide groups (HO−C═O/N−C═O) and to the oxygen of OH acid groups.[26,27]

A simple calculation, based on the attenuation of the gold substrate signal, leads to the average layer thicknesses of 5, 6, and 7 Å after 3, 30, and 60 min, respectively.

The increase of the 1600−1800 cm^{-1} IR absorption region and that of the average thickness, calculated from the gold peak attenuation, are reported in the graphs of parts a and b of Figure 9, respectively, for the three considered molecules.

Figure 4a shows the LEED pattern recorded at 25 eV obtained for the Au(110) surface exposed during 3 min to Gly-Pro. A detailed analysis of this diagram corresponds to a (6 0, 0 3) matrix. A LEED pattern is observed for 30 s up to 4 min of exposure to Gly-Pro. The diagram becomes less sharp after a few minutes of observation.

IGF on Au(110). Figure 5 shows the PM-RAIR spectra obtained upon increasing exposure of IGF on Au(110) surface at 300 K ($P_{Dose} = 1 \times 10^{-9}$ Torr). Clear IR bands can be observed from 5 min of exposure. The main features, summarized in Table 1, can be ascribed to vibrations arising from the constituent amino acid functionalities in addition to the amide I and II vibrations, indicating that IGF seems to be adsorbed intact at the surface.

With increasing coverage, the area of the spectral region including the $\nu_{C=O}$ at 1743 cm^{-1} and the amide I at 1666 cm^{-1} grows into two broad and very intense bands enveloping other vibrations like the asymmetric deformation of NH_3^+ at 1631 cm^{-1} and a weak asymmetric stretching mode of COO^- at 1590 cm^{-1}. In the 1500−1400 cm^{-1} region, a broad peak is observed, including the CH_2 scissor of the aliphatic ring of proline at 1488 cm^{-1},[19] the deformation band of the CH_2 chain at 1442 cm^{-1},[28] and the symmetric stretching mode of the COO^- at 1415 cm^{-1}. One can also identify the symmetric deformation of NH_3^+ at 1527 cm^{-1} and the amide II band at 1554 cm^{-1}, but these bands have very low intensities.

Figure 6 shows the C1s, N1s, and O1s XPS regions of the Au(110) surface after increasing exposure of IGF. Similarly to the case of Gly-Pro adsorption, with increasing coverage there seems to be a shift of the carbon, nitrogen, and oxygen peaks, but not for the gold one. The same type of recalibration used for Gly-Pro was operated. The C1s peak was best fitted with four contributions, shifted by ca. by 0.6 eV after 25 min and by 1.0 eV after 60 min, to get the COOH/CON O1s contribution at the expected value of 531.7 eV; the contributions at 284.9 ± 0.1, 286.0 ± 0.1, 287.9 ± 0.1, and 288.9 ± 0.1 eV can be reasonably assigned to the carbon atoms in CC or CH, CN, N−C═O or COO^-, and COOH groups, respectively.[24] With such a decomposition, a small contribution appears at ca. 283.3 eV that cannot be explained but by a differential charging effect within the IGF layer.

Applying the same correction onto the N1s peak, three contributions show up at 398.7 ± 0.1, 400.0 ± 0.1, and 401.3 ± 0.1 eV. The two contributions 400.0 and 401.3 eV are

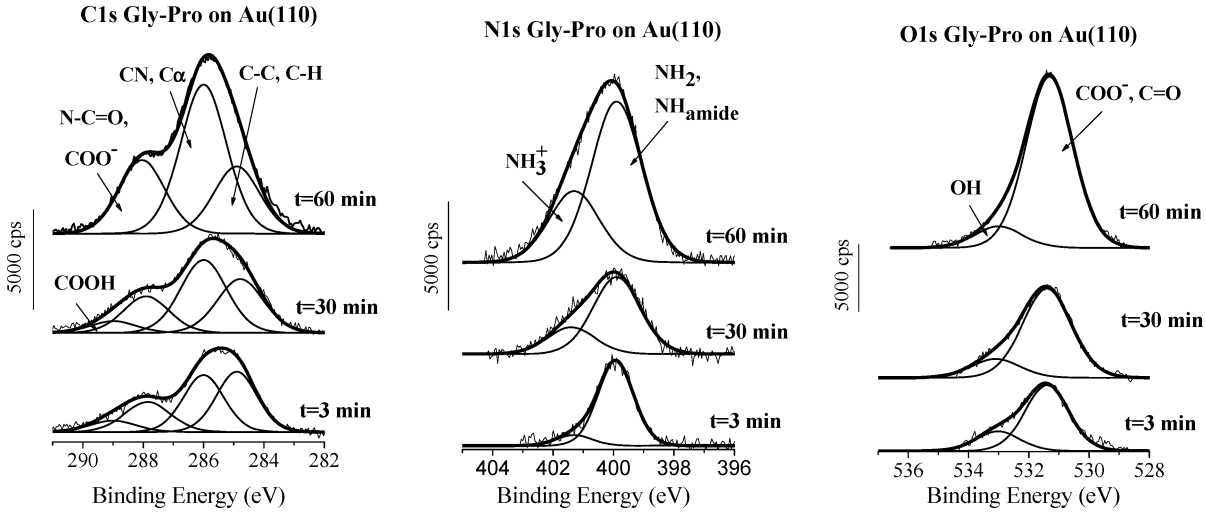

Figure 3. C1s, N1s, and O1s XPS high-resolution spectra recorded after adsorption of Gly-Pro during 3, 30, and 60 min on Au(110).

TABLE 2: XPS Binding Energies and Atomic Percentage of Gly-Pro/Au(110)

			experimental (atom %)			
element	assignment	BE (eV)	3 min	30 min	60 min	calculated (atom %)
C1s			67.1	63.9	62.3	58.3
	C−C/C−H	284.9	36.8	30.8	23.2	
	Cα, C−N	286	34.7	41.8	51.4	
	N−C═O, COO−	287.8	20.7	20.7	25.4	
	C(−OOH)	288.9	7.8	6.6		
N1s			11.3	12.9	15.7	16.6
	NH_2, NH_{amide}, R_3N	399.9	84	74.1	69.3	
	NH_3^+	401.3	16	25.9	30.7	
O1s			21.6	23.2	21.9	25.1
	COO^-, NHC═*O*, or/and HOC═*O*	531.4	77	82.5	88.8	
	CO*O*H	533	23	17.5	11.2	

attributed, respectively to N−H, tertiary N, or NH_2 groups and to the NH_3^+ group.[29] The third one, at a low binding energy of 398.7 ± 0.1 eV, is more difficult to assign; being at too low a binding energy to be the ternary nitrogen, it is more likely due to a N atom in strong interaction with Au.[30,31] Note that such an apparently low BE (binding energy) could be explained by a differential charging, like for the C1s peak; however, the rather high intensity of this low BE N1s peak is not consistent with that of the low BE C1s peak. One must admit that, in addition to the differential charge, a chemical effect contributes to yield such an intense peak at very low BE, this will be discussed later.

All XPS these data are summarized in Table 3.

As for the O1s peak, it was decomposed into two contributions, at 531.7 ± 0.1 and 533.2 ± 0.1 eV, attributed to the oxygen in C═O and O−H bonds, respectively; their relative proportions do not vary significantly upon increasing the surface coverage.

Finally, the average thickness layer, calculated from the ratio of C1s to Au4f intensities, increases strongly from 6 Å after 45 s to 28 Å after 60 min of exposure.

Figure 4b shows the LEED pattern recorded at 12 eV on the Au(110) exposed during 45 s under IGF. Adsorption leads to a 2D organization at this low coverage with a (5 2, −3 2) matrix; note that the diagram becomes fader after a few seconds of exposure to the LEED beam, suggesting a certain fragility of the locally ordered domains. No LEED pattern could be observed after longer exposure, suggesting a less strongly binding mode than the one observed previously for Gly-Pro.

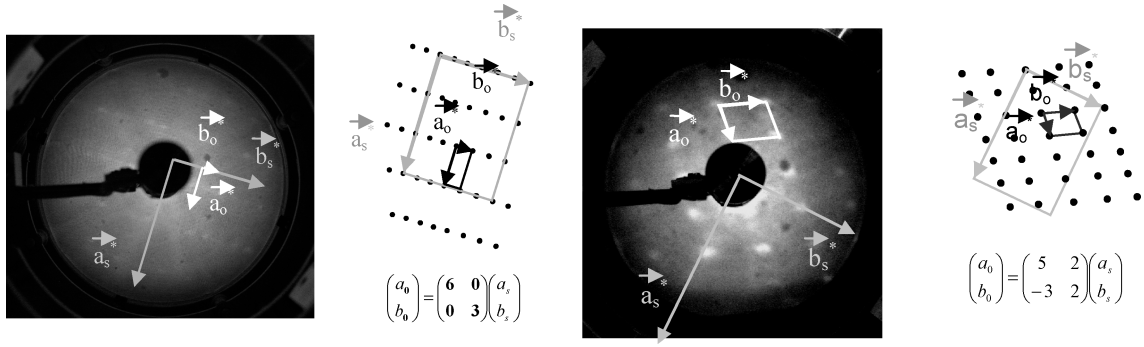

Figure 4. LEED pattern (a) recorded at 25 eV for a low-coverage phase of Gly-Pro on Au(110) and (b) recorded at 12 eV for a low-coverage phase IGF on Au(110).

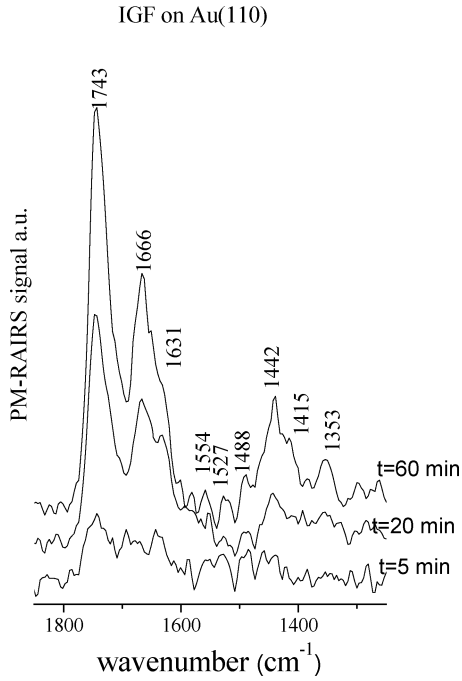

Figure 5. PM-RAIR spectra recorded upon increasing exposure of IGF at 300 K on Au(110).

GSH on Au(110). PM-RAIR spectra, obtained for GSH on Au(110) from 5 min of exposure up to 60 min, are shown in Figure 7. The main assignments are summarized in Table 1. There is no change in band positions upon further GSH exposure, and all bands can be correlated to the functionalities of the GSH. However, the relative intensities of these bands change with the coverage.

At high coverage, the band at 1697 cm^{-1}, which likely includes two contributions, the stretching mode of C═O in H-bonded carboxylic acid groups[15,18,32] and the free amide I signal,[8,9] becomes very predominant. Note also the presence of a strong shoulder peak at 1731 cm^{-1}, for the C═O of free acid groups.

Figure 8 shows the corresponding C1s, N1s, O1s, and S2p high-resolution XPS regions. Unlike, the two precedent systems Gly-Pro/Au(110) and IGF/Au(110), GSH adsorbed on Au(110) does not induce any charging effect, even at high coverage.

The C1s peak of GSH may be decomposed into the same four contributions as previously used for IGF on Au(110). Like on the IGF spectra, after 25 min of exposure, the C1s peak is dominated by the C−N, C_α (in a α position of the C═O group) contribution, as expected for that molecule. The N1s spectrum consists of two peaks at 399.9 ± 0.1 and 401.3 ± 0.1 eV corresponding, respectively, to amine or amide and to protonated amine nitrogen atoms.

The O1s peak presents two contributions at 531.7 ± 0.1 and 533.2 ± 0.1 eV are attributed, respectively, to the double-bonded oxygen of acidic and amide groups and to the oxygen of OH acid groups.[26,27] The OH fraction increases with the coverage, in agreement with the highest BE C1s contribution of the COOH component. These features indicate that more GSH molecules are under a fully neutral form; this is exactly opposite to the Gly-Pro and IGF behaviors.

Special attention was given to the S2p peak of the adsorbed GSH molecule: after 45 s of exposure, the S2p peak may be decomposed into only one doublet with the component $S2p_{3/2}$ at 162.1 ± 0.1 eV, assigned to sulfur bonded to Au. At that very low exposure,[33–35] GSH is chemisorbed on the gold surface via the sulfur atom of the cystein fragment. When the coverage increases, a new doublet appears on the S2p peaks of GSH, with an additional component $S2p_{3/2}$ at 164.1 ± 0.1 eV. This doublet, assigned to unbounded sulfur or SH, increases with the exposure time from 22% of the total S2p peak at 5 min up to 62% after 60 min. Some GSH molecules are now bound to the surface by another type of interaction.

Table 4 summarizes the XPS results obtained for the GSH adsorbed on Au(110).

No LEED image was obtained for the GSH at low coverage, suggesting that there was no 2D organization of the overlayer.

Discussion

A dipeptide, Gly-Pro, and two tripeptides, IGF and GSH, have been successfully deposited on Au(110) under UHV conditions and characterized by PM-RAIRS and XPS, which give complementary information about the kinetics of adsorption, the chemical form of the adsorbed molecules, as well as on the type of Au−molecule interaction.

For either of the three studied molecules, the surface coverage regularly increases from 45 s up to 60 min of exposure at ca. $P_{Dose} = 1 \times 10^{-9}$ Torr, with no net plateau in the PM-RAIRS or XPS characteristic intensities, suggesting a rather heterogeneous growth of the layers.

The kinetics of adsorption, in term of average thickness layer, increases in the following order (cf. Figure 9): Gly-Pro < GSH < IGF.

One notes that the total amount of organic material, after Gly-Pro adsorption, is less than half that obtained when adsorbing IGF under similar conditions, as would have been expected from the molecule formula, and this is more and more visible when increasing the exposure. This suggests that the additional fragments of the IGF molecule, compared to Gly-Pro, induce a stronger interaction with the surface, likely due to several centers of the molecule, and thus an increase of the number of adsorbed molecules under similar conditions.

All expected molecular groups have been identified on the surface by combining PM-RAIRS and XPS surface characterization; moreover, the atomic percentages, deduced from the XPS peaks, are very closed to the expected ones from each molecule formula, suggesting that all studied molecules adsorb intact on the surface.

Gly-Pro and the two tripeptides, IGF and GSH, mainly adopt a zwiterrionic form in the solid phase and likely exist under neutral forms in the gas phase, as observed for several amino acids.[36] All XPS and IR signals were carefully decomposed into contributions that were attributed to the likely existing groups, COO^-, COOH, NH_3^+, and NH_2. We then assumed that all molecules adsorb on the gold surface under globally neutral forms, which is most likely from an overview of the available results on amino acids on gold;[3,37] thus, two ionic forms have been considered for these two tripeptides, the zwiterrionic one $COOH/NH_3^+/COO^-$ and the neutral one $COOH/NH_2/COOH$; we will see that the extent of pronotation/deprotonation very much depends on the molecule.

Adsorption of Gly-Pro. From the very first stages of adsorption, the Au(110) surface gets covered with a Gly-Pro molecular layer, up to a thickness equivalent to one compact monolayer, ca. 5 Å, after already 3 min. For longer exposure, the amount of adsorbed Gly-Pro molecules still increases, probably as a multilayer in some places and, at that stage, probably involving electrostatic interactions between molecules, as suggested by the increasing fraction of molecules under a zwitterionic form.

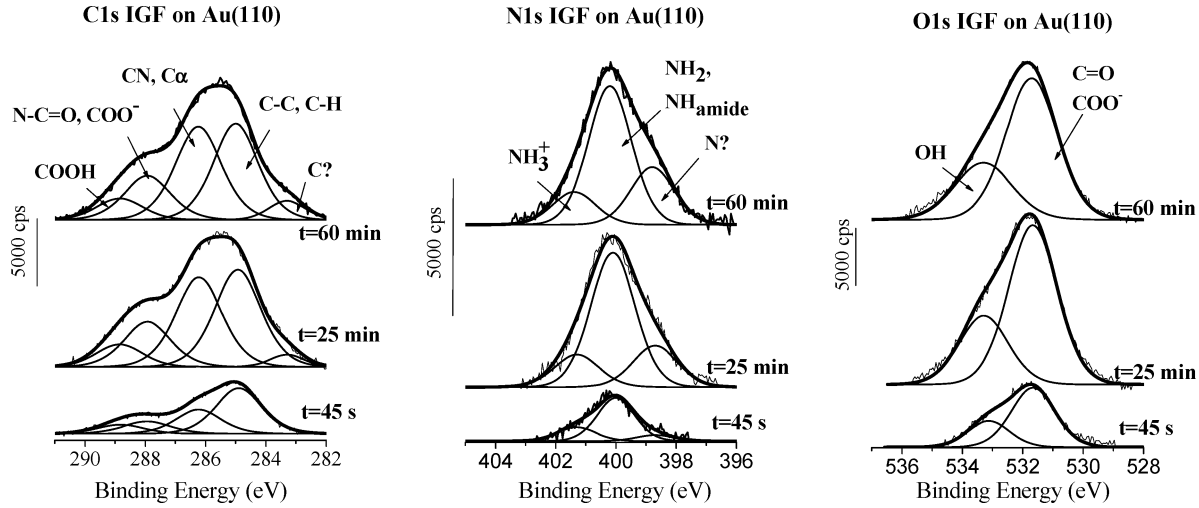

Figure 6. C1s, N1s, and O1s XPS high-resolution spectra recorded after adsorption of IGF during 5, 20, and 60 min on Au(110).

TABLE 3: XPS Binding Energies and Atomic Percentage of IGF/Au(110)

element	assignment	BE (eV)	experimental (atom %) 45 s	25 min	60 min	calculated (atom %)
C1s			64.84	61.25	61.9	57.1
	C?	283.3		3.3	5.5	
	C−C/C−H	284.9	50.2	37	35	
	Cα, C−N	286.2	26.2	34.2	35.1	
	N−C═O, COO^-	287.9	13.8	17.2	16.6	
	C(−OOH)	288.9	9.8	8.3	7.8	
N1s			10.6	13.4	14.5	14.3
	N?	398.7	9.5	20	25.2	
	NH_2, NH_{amide}, R_3N	400	68.4	64.5	60.5	
	NH_3^+	401.3	22.2	15.6	14.3	
O1s			24.5	25.3	23.6	28.6
	COO^-, NHC═*O*, or/and HOC═*O*	531.7	70.9	69.8	71.3	
	CO*O*H	533.2	29.1	30.2	28.7	

As a matter of fact, from the contribution of NH_3^+, one calculates the proportion of zwitterionic and neutral Gly-Pro forms for the different times of exposure. The proportion of zwitterionic Gly-Pro form increases from 32% after 3 min to 60% after 60 min. Moreover, the proportion of OH contribution on the O1s XPS peak decreases strongly with the increasing exposure; this together with the very low intensity of the $\nu_{C=O}$ in PM-RAIR spectra confirms that the proportion of zwitterionic Gly-Pro molecules increases with the coverage.

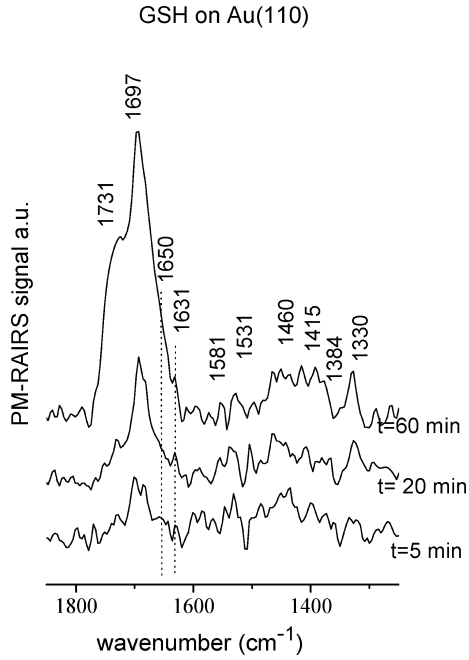

Figure 7. PM-RAIR spectra recorded upon increasing GSH exposure at 300 K on Au(110).

Note that the PM-RAIR spectra also show a very weak C═O stretch band, especially after 60 min of adsorption, though ca. one-third of the molecules should still be under a fully neutral form; this may be due to the unfavorable orientation of the Gly-Pro molecules. The slight charging effect, observed on the XP spectra, confirms the growth of a rather uniform, nonconducting monolayer, followed by growth of thicker patches or multilayers.

This is also in agreement with the observation of a rather ordered initial layer giving rise to some 2D organization detected by LEED.

Adsorption of IGF. The adsorption of IGF on Au(110) is rapid and continuous up to 60 min, without suggesting any saturation or plateau. The 2D organization observed by LEED, in addition to the charging effect on the XPS spectra, suggests a rather continuous, rapidly formed layer of IGF, followed by a layer-by-layer growth of the isolating organic layer.

As in the case of Gly-Pro adsorbed on Au(110), the presence of features attributed to the carboxylic acid, carboxylate, NH_2, and NH_3^+ species on the PM-RAIR spectra, shows that the ionic and fully neutral forms of IGF coexist on the surface. It is more difficult to appreciate their relative amounts from the XPS N1s region, the interpretation of which requires some discussion. A

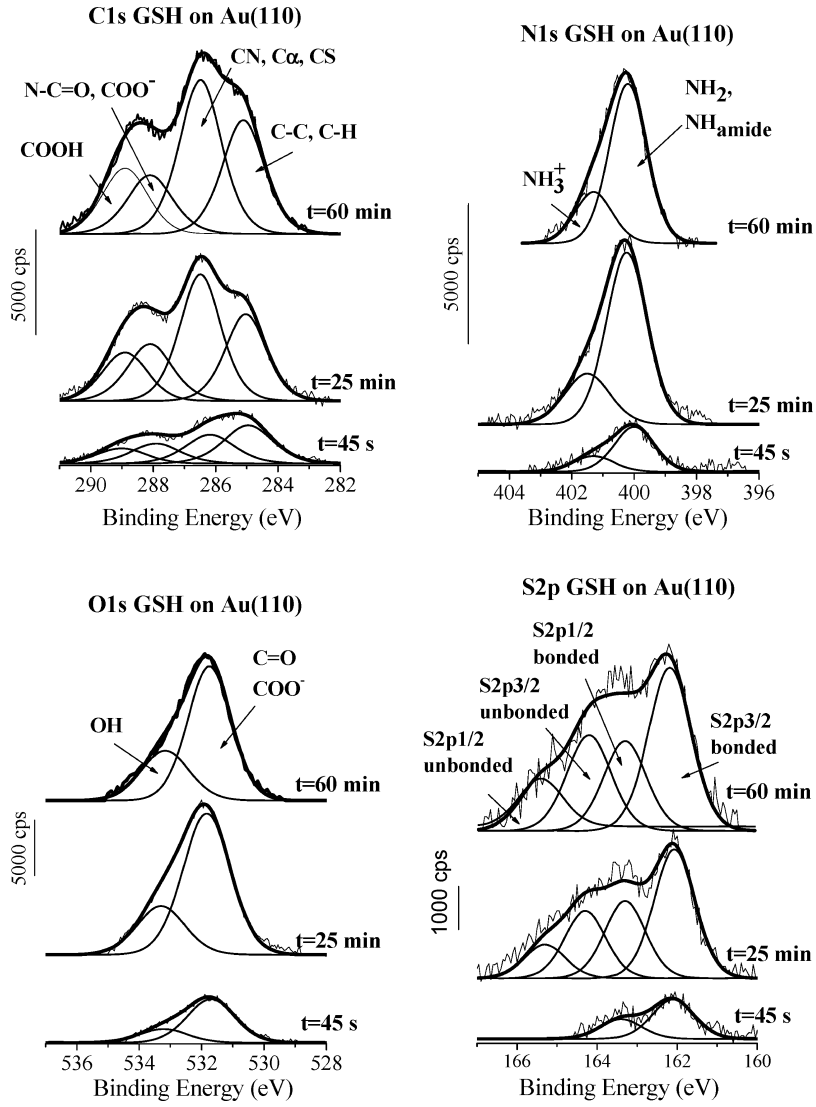

Figure 8. C1s, N1s, O1s, and S2p XPS high-resolution spectra recorded after adsorption of GSH during 5, 20, and 60 min on Au(110).

differential charging effect is obvious on the C1s spectra (25 or 60 min exposure); thus, it could explain the presence of a N1s peak at very low BE, i.e. 398.7 eV; however, the relatively high intensity of the latter implies an additional chemical effect. We may attribute such a low BE contribution to a nitrogen atom bound to gold with a significant electron transfer. We rather believe that IGF forms very strong bonds with gold, and this may occur via the central NH group, the ternary amine, or the glycine side terminal NH_2. The two latter cases would also occur in the adsorption of Gly-Pro and lead to the same nitrogen peak; it is thus unlikely. The former type of interaction would indeed lead to a quasiternary nitrogen interacting with the metal surface, which is indeed a possibility with such a molecule.

Though the calculation of the proportion of zwiterrionic and fully neutral IGF molecules from the contribution of NH_3^+ is difficult, one may however observe that, conversely to what was seen for Gly-Pro, the COOH and NH_3^+ relative contributions seem almost constant or only slightly increase with exposure. In other words, from the very beginning of the interaction, some IGF molecules adopt a zwitterionic form on the surface.

Note that the PM-RAIR spectra are all dominated by the C═O stretch of acid groups; the molecule has two of them, one being likely partially deprotonated and the other one remaining under the COOH form.

Adsorption of GSH. GSH also adsorbs on the Au(110) surface under low pressure ($P_{Dose} = 1 \times 10^{-9}$ Torr). For this molecule, the S2p peak was recorded and appeared to be very informative: at low coverage, the single sulfur doublet is proof of the binding of GSH via its S atom, while, at higher coverage, the presence of a doublet to the high BE side of the S2p peak reveals the presence of unbound sulfur, suggesting that molecules are not any longer interacting via the thiol group: 22% after 5 min of exposure and up to 62% after 60 min of exposure. The PM-RAIR spectra are dominated by a broad band in the 1650−1740 cm^{-1} region. The higher wavenumber contribution is due to the C═O stretching band of the isolated carboxyl groups, while that at ca. 1697 cm^{-1} may be reasonably attributed to the C═O stretch of H-bonded carboxyl groups; this clearly suggests the formation of acid dimers, in agreement with the presence of unbound sulfur. The formation of GSH dimers, already evidenced on the Au(111) surface, under similar conditions,[15] may also explain the absence of any 2D organization and of any charging effect, since the surface is covered by heterogeneous clusters of GSH rather by an homogeneous organic layer. The growth of GSH layers under the form of dimers or clusters, leading to an incomplete coverage of the Au layer, constitutes the main difference with the growth of IGF layers.

TABLE 4: XPS Binding Energies and Atomic Percentage of GSH/Au(110)

element	assignment	BE(eV)	experimental (atom %) 45 s	25 min	60 min	calculated (atom %)
C1s			59.3	52.5	56.7	56.6
	C−C/C−H	284.9	37.5	26.5	28.5	
	Cα, C−N, C−S	286.0	28.3	35.1	38.5	
	N−*C*═O, COO^-	287.8	19.6	16.4	15.8	
	C(−OOH)	288.9	14.6	16.7	17.2	
N1s			14	16.5	13.3	13.7
	NH_2, NH_{amide}, R_3N	399.9	74	75.3	75.7	
	NH_3^+	401.3	26	24.7	24.3	
O1s			23.5	25.7	24	23.9
	COO^-, NHC═*O*, or/and HOC═*O*	531.4	76	74.3	70.9	
	CO*O*H	533.0	24	25.7	29.1	
S2p			3.3	5.3	6	5.8
	$S2p_{3/2}$ bonded	162.1	66.7	41.9	40.7	
	$S2p_{1/2}$ bonded	163.3	33.3	25.1	22.4	
	$S2p_{3/2}$ unbonded	164.1	−	21.9	24.6	
	$S2p_{1/2}$ unbonded	165.3	−	11	12.3	

The proportion of zwitterionic and neutral forms for the different exposure times is deduced from the NH_3^+ contribution. The proportion of zwitterionic forms goes from about 78% at very low coverage down to 74% at 60 min. This high proportion of zwitterionic GSH form is in agreement with the high number of H-bonded interactions present from the early stages of adsorption.

Growth Mode Comparison. The evolutions of the PM-RAIR spectra of GSH and IGF on Au(110) (cf. Figure 9) show an increase of the number of adsorbed molecules with the exposure time, the PM-RAIRS area increase being more rapid for IGF than for GSH. This comparison does not take into account the orientations of the IR-active groups that may enhance some signals and induce some errors in the correlation between IR intensities and the number of adsobates. We, however, consider that, on average, the spectral zone considered in Figure 9, including signals from at least four dipole moments, $\nu_{C=O}$ (amide or acid groups), $\nu_{asymCOO-}$, and δ_{NH_2}, provides a reasonable indication of the relative amounts of adsorbed molecules. The evolution of the average thickness deduced from the Au4f attenuation shows the same trend. In the case of IGF, the average thickness increases from 6 Å after 45 s up to 20 Å after 60 min, while in the case of GSH the average thickness increases more slowly from 5 Å after 45 s up to 13 Å after 60 min; the PM-RAIRS data enable us to say that, for equivalent molecular sizes, IGF is adsorbed in an amount roughly twice greater than of GSH, under similar conditions. These values must be considered with caution; they only provide an estimation of the thickness layers if the latter are homogeneously dispersed, which is obviously not the case. The graph of Figure 9 (lower part) is however a reliable indication when comparing the total amounts of molecules contributing to the gold attenuation. Moreover, the LEED pattern of the IGF highlights the presence of ordered adlayer at low coverage, while no LEED pattern is obtained for GSH. This is of course related to their different modes of interaction. One sees the determining influence of the presence of a thiol group on the molecule: it governs the adsorption from the beginning of exposure, and then, surprisingly, the formation of dimers is preferred, likely because, for geometric reasons, H-bonds between $COOH/NH_2/CONH$ groups, in between different GSH molecules, are possible and prevail over a completion of the layer.

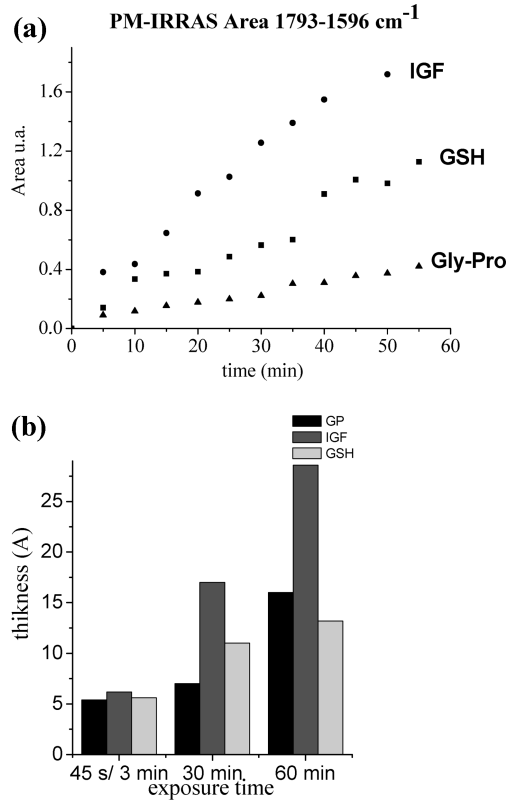

Figure 9. (a) Evolutions of the PM-RAIRS area in the 1793−1596 cm^{-1} region of GSH, IGF, and Gly-Pro on Au(110) under exposure. (b) Evolution of the GSH, IGF. and Gly-Pro thickness, calculated from the XPS data at various exposure times.

At the beginning of the adsorption, the Gly-Pro and IGF are both adsorbed on the surface with an ordered phase observed on the LEED patterns. These two peptides seem to grow first under a full monolayer and then, when the coverage increases, aggregates of IGF are probably formed, as suggested by the observed differential charge effect on the C1s and N1s XPS data. This is not the case for Gly-Pro. The size of the peptide and the presence of more COOH groups influence its growth mode.

Conclusion

Rather big molecules, ($m \sim 300$ g mol^{-1}) may be adsorbed under UHV by sublimation and permit the in situ characterization of surfaces at increasing coverage values.

By adsorbing two tripeptides, IGF and GSH, and one related-dipeptide on Au(110) under UHV conditions, original surface

PM-RAIRS and XPS data were obtained that unraveled some interesting tendencies, with some clear differences, induced by only slight variations in the molecular formula.

IGF and Gly-Pro, two molecules differing by an additional glutamic acid moiety on the first one, strongly interact with the gold surface, likely via NH_2 and also COOH groups if the geometry permits it. It gives rise to some 2D organization and a rather homogeneous adlayer. Conversely, the adsorption of GSH, bearing a thiol group, occurs in two phases: a preferential interaction via the SH group rapidly followed by the formation of dimers on the surface rather than a homogeneous layer. In other words, intermolecular H-bonds prevail over the full covering of the surface via S−Au or other interactions. These kinetics and structural new results may be of importance for some applications in the domain of biocompatibility or biorecognition.

PM-RAIRS and XPS techniques appear to be very complementary and informative for the basic understanding of these complex molecular layers.

References and Notes

(1) Kasemo, B. *Surf. Sci.* **2002**, *500*, 656.

(2) Ihs, A.; Liedberg, B.; Uvdal, K.; Törnkvist, C.; Bodö, P.; Lundström, I. *J. Colloid Interface Sci.* **1990**, *140*, 192.

(3) Uvdal, K.; Bodö, P.; Liedberg, B. *J. Colloid Interface Sci.* **1992**, *149*, 162.

(4) Hasselström, J.; Karis, O.; Weinelt, M.; Wassdahl, N.; Nilsson, A.; Nyberg, M.; Pettersson, L. G. M.; Samant, M. G.; Stöhr, J. *Surf. Sci.* **1998**, *407*, 221.

(5) Kühnle, A.; Linderoth Trolle, R.; Hammer, B.; Besenbacher, F. *Nature (London)* **2002**, *415*, 891.

(6) Barlow, S. M.; Raval, R. *Surf. Sci. Rep.* **2003**, *50*, 201.

(7) Humblot, V.; Haq, S.; Muryn, C.; Hofer, W. A.; Raval, R. *J. Am. Chem. Soc.* **2002**, *124*, 503.

(8) Ataka, S.; Takeuchi, H.; Tasumi, M. *J. Mol. Struct.* **1984**, *113*, 147.

(9) Törnkvist, C.; Liedberg, B.; Lundström, I. *Langmuir* **1991**, *7*, 479.

(10) Iucci, G.; Battocchio, C.; Dettin, M.; Gambaretto, R.; Di Bello, C.; Borgatti, F.; Carravetta, V.; Monti, S.; Polzonetti, G. *Surf. Sci.* **2007**, *601*, 3843.

(11) Polzonetti, G.; Battocchio, C.; Dettin, M.; Gambaretto, R.; Di Bello, C.; Carravetta, V.; Monti, S.; Iucci, G. *Mater. Sci. Eng., C* **2008**, *28*, 309.

(12) Valdes, T. I.; Ciridon, W.; Ratner, B. D.; Bryers, J. D. *Biomaterials* **2008**, *29*, 1356.

(13) Barlow, S. M.; Haq, S.; Raval, R. *Langmuir* **2001**, *17*, 3292.

(14) Wang, Y.; Lingenfelder, M.; Classen, T.; Costantini, G.; Kern, K. *J. Am. Chem. Soc.* **2007**, *129*, 15742.

(15) Vallée, A.; Humblot, V.; Methivier, C.; Pradier, C.-M. *Surf. Sci.* **2008**, *602*, 2256.

(16) Vallée, A.; Humblot, V.; Méthivier, C.; Pradier, C.-M. *Surf. Interface Anal.* **2008**, *40*, 395.

(17) Scofield, J. H. *J. Electron Spectrosc. Relat. Phenom.* **1976**, *8*, 129.

(18) Jones, T. E.; Baddeley, C. J. *Surf. Sci.* **2002**, *513*, 453.

(19) Marti, E. M.; Barlow, S. M.; Haq, S.; Raval, R. *Surf. Sci.* **2002**, *501*, 191.

(20) Marti, E. M.; Methivier, C.; Pradier, C. M. *Langmuir* **2004**, *20*, 10223.

(21) Barlow, S. M.; Kitching, K. J.; Haq, S.; Richardson, N. V. *Surf. Sci.* **1998**, *401*, 322.

(22) Efstathiou, V.; Woodruff, D. P. *Surf. Sci.* **2003**, *531*, 304.

(23) Gao, F.; Wang, Y.; Burkholder, L.; Tysoe, W. T. *Surf. Sci.* **2007**, *601*, 3579.

(24) Beamson, G.; Briggs, D. *The XPS of Polymers Database*; SurfaceSpectra: Manchester, UK, 2000.

(25) Uvdal, K.; Bodö, P.; Ihs, A.; Liedberg, B.; Salaneck, W. R. *J. Colloid Interface Sci.* **1990**, *140*, 207.

(26) Han, S. W.; Joo, S. W.; Ha, T. H.; Kim, Y.; Kim, K. *J. Phys. Chem. B* **2000**, *104*, 11987.

(27) Polzonetti, G.; Battocchio, C.; Iucci, G.; Dettin, M.; Gambaretto, R.; Di Bello, C.; Carravetta, V. *Mater. Sci. Eng., C* **2006**, *26*, 929.

(28) Jones, T. E.; Urquhart, M. E.; Baddeley, C. J. *Surf. Sci.* **2005**, *587*, 69.

(29) Fleming, G. J.; Adib, K.; Rodriguez, J. A.; Barteau, M. A.; Idriss, H. *Surf. Sci.* **2007**, *601*, 5726.

(30) Inamura, K.; Inoue, Y.; Ikeda, S.; Kishi, K. *Surf. Sci.* **1985**, *155*, 173.

(31) Petrovykh, D. Y.; Kimura-Suda, H.; Whitman, L. J.; Tarlov, M. J. *J. Am. Chem. Soc.* **2003**, *125*, 5219.

(32) Humblot, V.; Haq, S.; Muryn, C.; Raval, R. *J. Catal.* **2004**, *228*, 130.

(33) Castner, D. G.; Hinds, K.; Grainger, D. W. *Langmuir* **1996**, *12*, 5083.

(34) Dodero, G.; De Michieli, L.; Cavalleri, O.; Rolandi, R.; Oliveri, L.; Dacca, A.; Parodi, R. *Colloids Surf., A* **2000**, *175*, 121.

(35) Beerbom, M. M.; Gargagliano, R.; Schlaf, R. *Langmuir* **2005**, *21*, 3551.

(36) Shin, T.; Kim, K.-N.; Lee, C.-W.; Shin, S. K.; Kang, H. *J. Phys. Chem. B* **2003**, *107*, 11674.

(37) Gonella, G.; Terreni, S.; Cvetko, D.; Cossaro, A.; Mattera, L.; Cavalleri, O.; Rolandi, R.; Morgante, A.; Floreano, L.; Canepa, M. *J. Phys. Chem. B* **2005**, *109*, 18003.

JP9003888